



VitroMinerals
SUSTAINABLE GLASS POWDERS

VCAS™ White Pozzolans

Properties of concrete containing vitreous calcium aluminosilicate pozzolan



VitroMinerals
SUSTAINABLE GLASS POWDERS

Address: 9126B Industrial Blvd., Covington, GA, 30014
Phone: 678-729-9333 / Fax: 678-729-9336

www.vitrominerals.com
technicalsales@vitrominerals.com

**PROPERTIES OF CONCRETE CONTAINING VITREOUS CALCIUM
ALUMINOSILICATE POZZOLAN**

Satiar A. Shirazi
Undergraduate Assistant
Department of Civil Engineering
University of South Alabama
Mobile, AL 36688
Email: saa310@jaguar1.usouthal.edu
Phone: 251-460-6174
Fax: 251-461-1400

Akhter B. Hossain (Corresponding Author)
Assistant Professor
Department of Civil Engineering
University of South Alabama
Mobile, AL 36688
Email: ahossain@jaguar1.usouthal.edu
Phone: 251-460-7438
Fax: 251-461-1400

Jarrod Persun
Undergraduate Assistant
Department of Civil and Environmental Engineering
Clarkson University, Box. 5710
Potsdam, NY 13699
E-mail: persunjd@clarkson.edu
Phone: 315- 268-7701
Fax: 315- 268-7985

Narayanan Neithalath
Assistant Professor
Department of Civil and Environmental Engineering
Clarkson University, Box. 5710
Potsdam, NY 13699
E-mail: nneithal@clarkson.edu
Phone: 315- 268-1261
Fax: 315- 268-7985

Number of Words: Abstract 218, Body 4350, 3 Tables, 9 Figures = **Total 7568**

87th Transportation Research Board Annual Meeting, January, 2008
Washington, DC

PROPERTIES OF CONCRETE CONTAINING VITREOUS CALCIUM ALUMINOSILICATE POZZOLAN

ABSTRACT

This paper describes a laboratory study on the influence vitreous calcium aluminosilicate (VCAS), a new pozzolanic mineral admixture, on the properties of fresh and hardened portland cement concrete. The paper provides a relative comparison of the performance of concrete containing VCAS with that of concrete containing silica fume (SF), which is one of the widely used mineral admixtures. It was observed that the addition of VCAS pozzolan increased the slump (improved consistency) of the mixtures, while the addition of SF decreased it. The VCAS pozzolan was found not to have significant influence on the plastic shrinkage cracking potential of the mixtures while SF increased it. The compressive strength development of both the VCAS and SF mixtures were found to be higher than that of the control mixture. The experimental results showed that both VCAS and SF increased the free shrinkage of concrete. The rapid chloride permeability (RCP) values for mixtures with VCAS and SF specimens were significantly lower than those of the control concrete. At equal replacements of cement with either VCAS or SF, the reduction in RCP values was higher for the SF modified mixtures. Incorporation of either VCAS or SF also reduced the sorptivity and moisture diffusion coefficient of the concrete mixtures. This study provides insight into the behavior of concretes containing two high-performance mineral admixtures.

INTRODUCTION

In recent years, high-performance concrete (HPC) has become widely used in transportation structures where strength and durability are two important considerations. In HPC, a part of portland cement is replaced by pozzolanic materials. These pozzolans improve the strength and durability of concrete (1,2,3), and the mechanisms by which these are accomplished are well known.

Among the various pozzolans used to enhance the performance of concrete, vitreous calcium aluminosilicate (VCAS) is a relatively new one. VCAS is a white pozzolanic material produced from glass fiber manufacturing waste. It is processed by grinding waste glass fibers to a fine powder form that effectively demonstrates pozzolanic behavior (4). VCAS pozzolan is white in color and very consistent in chemical composition because the waste fibers from glass industries are vitreous, clean, and low in iron and alkalis.

Since VCAS is a new pozzolanic admixture, relatively little information is available on various physical properties of concrete made with VCAS which would allow the development of comprehensive mixture proportioning procedures. This paper describes a study in which an attempt is made to investigate the influence of VCAS pozzolan on several important properties of fresh and hardened concrete. The paper provides a relative comparison of the performance of concrete containing VCAS with that of concrete containing silica fume (SF), which is one of the widely used mineral admixtures.

MATERIALS AND MIXTURE PROPORTIONS

In this study, a series of experiments was performed to investigate the influence of VCAS pozzolans on the properties of concrete. Several concrete mixtures were made with Type I cement, and VCAS, or SF as the binding materials. The VCAS pozzolan used in this study met all the performance specifications of ASTM C-618 and C-1240 (5). The specific gravity of the VCAS pozzolan was 2.6 and the mean particle size was 3 μm . A dry, densified form of SF was used in this study, which conforms to the requirements of ASTM C-1240 (5). Table 1 shows the chemical properties of VCAS and SF used in this study. Concrete mixtures were proportioned with water-binder ratios (w/b) of 0.40 and 0.50, and a combined aggregate volume of 65%. The pozzolans were added to the mixtures by replacing a portion of the cement by mass. The Plain mixture (control) did not contain any pozzolanic material and was used as the base line for comparison with other mixtures. Mixtures VCAS-6, VCAS-9 and VCAS-15 were prepared by replacing 6%, 9% and 15% of cement by mass in the mixtures respectively with VCAS. SF-6 and SF-9 mixtures were prepared by replacing 6% and 9% of cement by mass respectively with SF. The mixture proportions are shown in Table 2.

ABLE 1 Chemical Compositions of VCAS and SF

	SiO ₂ (%)	Al ₂ O ₃ (%)	Fe ₂ O ₃ (%)	CaO (%)	MgO (%)	SO ₃ (%)	Na ₂ O (%)	K ₂ O (%)	LOI (%)
VCAS	50-55	15-20	<1.0	20-25	<1.0	<0.1	<1.0	<0.2	<0.5
SF	93.4	0.42	0.52	1.91	-	0.34	0.25	0.79	2.3

TABLE 2 Mixture Proportions (units are in kg/m³)

Mix	Sand	Coarse Agg.	w/b = 0.40				w/b = 0.50			
			Cement	Water	VCAS	SF	Cement	Water	VCAS	SF
Plain	862	895	427	171	-	-	375	187	-	-
VCAS-6	860	894	402	171	26	-	352	187	22	-
VCAS-9	859	892	389	171	38	-	341	187	34	-
VCAS-12	857	890	363	171	64	-	318	187	56	-
SF-6	860	893	402	171	-	26	352	187	-	22
SF-9	859	891	389	171	-	38	341	187	-	34

EXPERIMENTAL PROCEDURE

The following parameters were used in this study to investigate the influence of VCAS on the properties of fresh and hardened concrete:

- slump,
- plastic shrinkage cracking,
- free shrinkage,
- compressive strength,
- rapid chloride permeability, and
- sorptivity and moisture diffusion coefficient.

The test methods used in this study are briefly described below.

The slump of fresh concrete mixtures was measured according to ASTM C-143 on concrete mixtures with a w/b of 0.50. No water reducer was used in these mixtures.

The plastic shrinkage cracking test was performed on three 0.50 w/b mixtures (Plain, VCAS-9 and SF-9). The restrained slab specimens similar to that used by Qi et al. (6, 7) were used, the geometry of which is shown in Fig.1. Two grips at the bottom of the slabs provide sufficient restraint at the base of the specimen, while a stress riser significantly reduces the slab depth at the center of the slab. Cracking is expected to occur above the stress riser across the width of the slab specimen. Immediately after mixing (approximately 30 minutes after the water was added to the mixture), the restrained slab specimens were transferred to an environmental chamber where they were exposed to a constant temperature of 100°F (37.7°C) and a relative humidity (RH) of 50%. In order to hasten the drying process, high velocity fans were used to blow wind on the top of the slab specimens. The wind velocity was approximately 24 km/h. The plastic shrinkage cracking test setup is shown in Fig. 2.

The free shrinkage strains of the concrete mixtures were determined in this study according to ASTM C-157. Three prisms were prepared for each concrete mixture. The prisms had 75 mm (3 in.) square cross sections and 250 mm (10 in.) gage lengths. The specimens were demolded and transferred to a constant RH (50%) and temperature (21° C) chamber approximately 24 hours after mixing and kept there throughout the duration of the experiment. The length change of each prism was measured using a digital comparator at frequent intervals. From the length changes, free shrinkage strains were calculated.

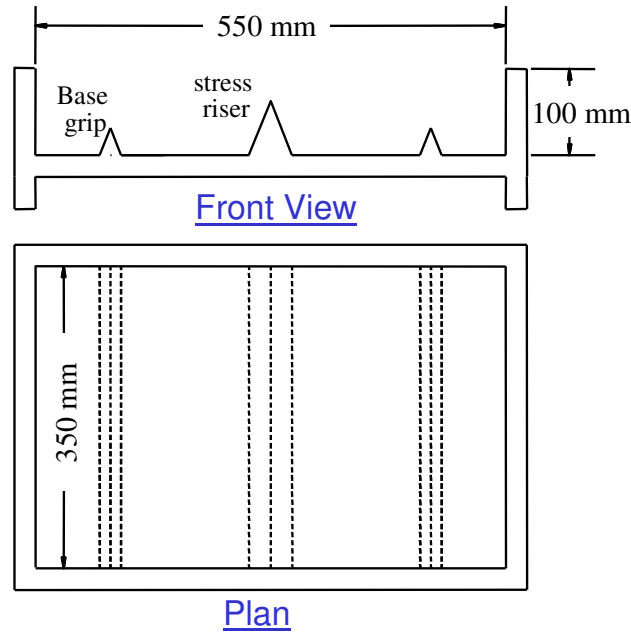


FIGURE 1 Restrained slab geometry.



FIGURE 2 Restrained shrinkage cracking test setup.

The compressive strength of the concrete mixtures was determined according to the ASTM C-39 method. Concrete cylinders with 200 mm (8 in.) height and 100 mm (4 in.) diameter were used to measure the compressive strength at 3, 7, 14, 28 and 56 days of curing.

The rapid chloride permeability test (RCPT) was carried out as per ASTM C 1202-07 on 0.40 w/b mixtures. 50 mm thick slices of concrete cut from 100 mm diameter cylinders which were moist cured for either 28 or 45 days were used. It should be noted that this test does not provide an indication of permeability or diffusivity directly, rather it is a measure of the concrete's resistance to ion penetration.

For the water transport experiments, the following specimen conditioning procedure was adopted. 50 mm thick specimens from 0.40 w/b mixtures were kept in an oven at $70 \pm 2^\circ\text{C}$ for 3 days after 28 days of moist curing. After their removal from the oven, these specimens

were cooled down to room temperature and placed in a closed container at room temperature for an additional 24 hours. Heating at 105° C as suggested by some authors (8, 9) was not adopted for these specimens to prevent microcracking, and thus to avoid the possibilities of obtaining unrealistically high sorptivity values. The water transport tests carried out in this study conforms to a RILEM recommendation (10). The specimens were sealed on their outer perimeter using electrical tape, and a small dyke was made on the top surface to retain water. The bottom surface of the specimen also was covered with tape. The initial mass of the specimen was measured and the top of the specimen was filled with water to a height of 15 mm above the specimen surface. The mass of the specimen was measured at regular intervals using a balance accurate to one hundredth of a gram. The amount of water taken in by the specimen (M) was calculated and normalized by the cross sectional area (A) exposed to water.

ANALYSIS AND RESULTS

The following sections deal with the analysis and discussion of the results obtained from the aforementioned tests designed to understand the influence of VCAS on properties of fresh and hardened concrete, and facilitate comparison with mixtures incorporating SF.

Slump of VCAS and SF Modified Concretes

The results of slump test are presented in Fig. 3. It should be noted that the slumps were measured on 0.50 w/b mixtures without any water reducing admixture. The average of three slump measurements for each concrete mixture is shown. It is evident from the figure that the addition of VCAS pozzolan increased the slump of the mixtures. An increase in slump indicates an improvement in mixture consistency and a reduction in water demand. On the other hand, addition of silica fume made the concrete mixtures stiffer, resulting in a reduction in workability as shown in the figure.

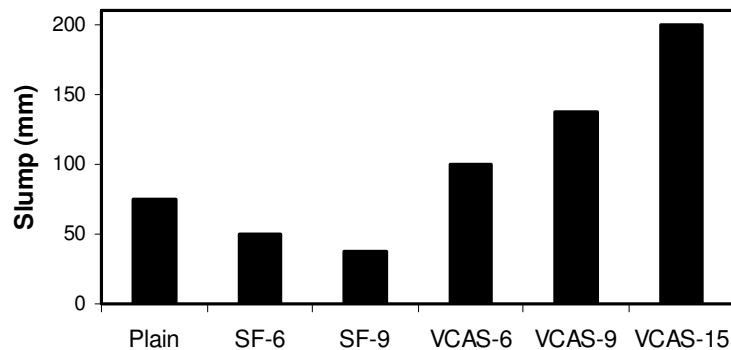


FIGURE 3 Slump of different concrete mixtures.

Plastic Shrinkage Cracking

The restrained slabs discussed in the earlier section were observed for cracks approximately at an age of 24 hours. It was found that all the specimens cracked along the length of the stress riser. To quantify cracking, an image analysis technique was used. The crack images on the surface of the specimens were captured using a CCD camera. The camera was mounted on a specially designed traveling frame. The image frame size was chosen in such a way that a 62.5 x 50 mm image would provide a resolution of 1280 x 1024 pixels (0.0488

mm/pixel), allowing a sensitivity of 0.0488 mm in crack width measurement. Each captured image was then processed using Image J software. The original images were converted to binary images and the crack contours were separated from the bulk concrete background using the gray level intensity (0 – black and 255 –white) of the individual pixels. The image capturing and processing procedure is illustrated in Fig. 4. Once the crack was separated, the crack area was determined using the known area of the individual pixels in the crack contour. The total crack area of each individual specimen was then expressed as a percentage of total drying area (550 x 350 sq. mm or 22 x 14 sq. in.) of the specimens as shown in Eq. 1.

$$\text{Crack Area (\%)} = \frac{\text{Area of the crack}}{\text{Total drying area of the specimen}} \cdot 100 \quad (1)$$

In addition to the crack area (%), the plastic shrinkage cracking potential (Eq. 2) was estimated following a procedure similar to Garon et al. (11). According to this procedure, the cracking potential is the ratio of the crack area in the specimens containing pozzolans (A_{CP}) to that in the plain (control) specimen (A_{CC}).

$$\text{Cracking Potential} = \frac{A_{cp}}{A_{cc}} \quad (2)$$

The results of three sets of plastic shrinkage cracking tests (Tests 1, 2 and 3) are shown in Fig. 5. In each test set, the Plain, VACS-9 and SF-9 mixtures with w/b of 0.50 were used. From Fig. 5(a) it is evident that in all test sets, the SF specimens had the highest crack area. There is no significant difference between the crack areas in plain and VCAS specimens. The plastic shrinkage cracking potentials of the concrete mixtures used in this test are shown in Fig. 5(b). It can be clearly noticed that the addition of VCAS pozzolan did not significantly influence the plastic shrinkage cracking potential of the mixtures while the addition of silica fume significantly increased it.

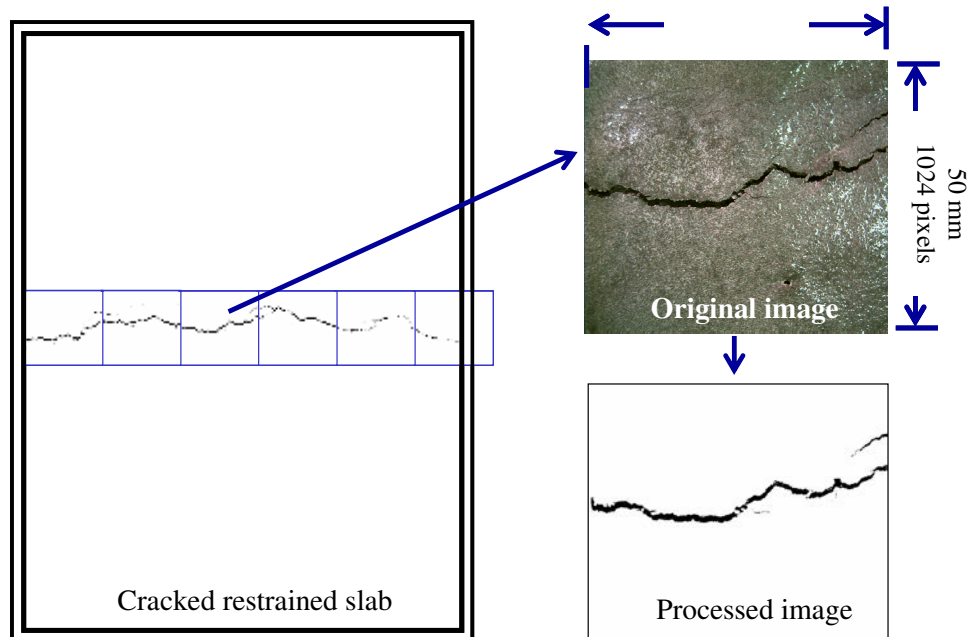
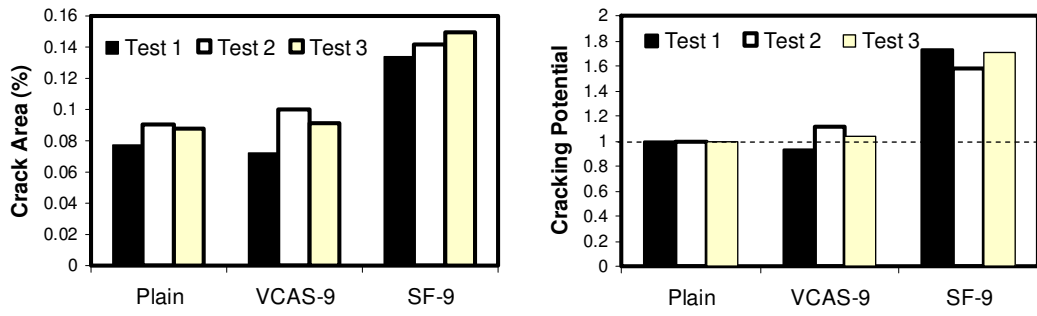
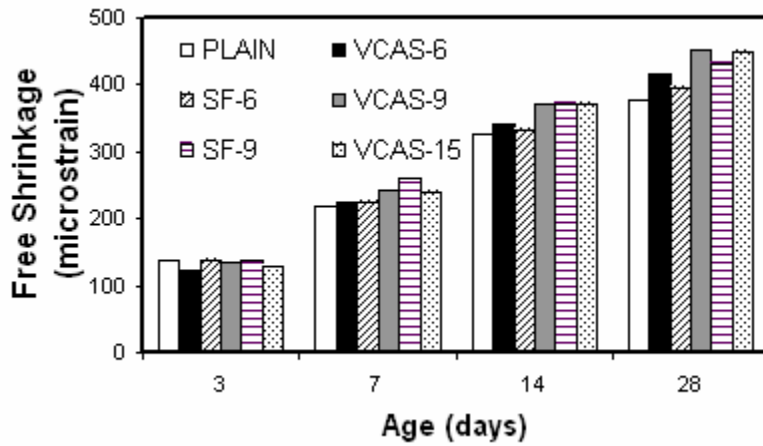


FIGURE 4 Crack image capture and processing.

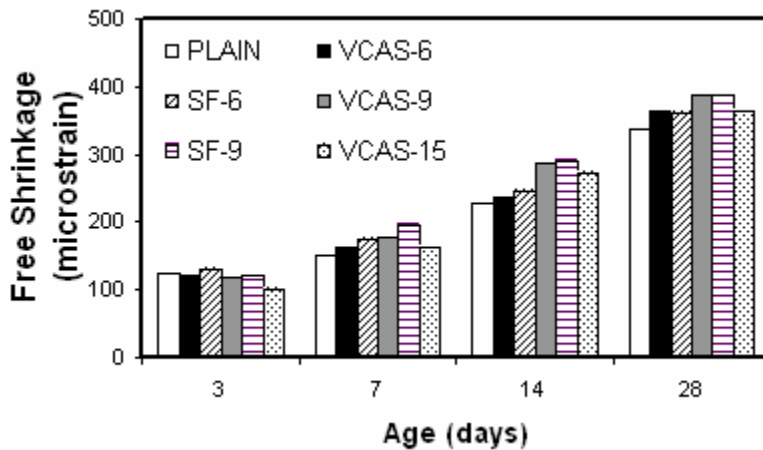


(a) Crack area expressed as a percentage of total area (b) Plastic shrinkage cracking potential

FIGURE 5 Plastic shrinkage crack area and cracking potential.



(a) w/b = 0.40

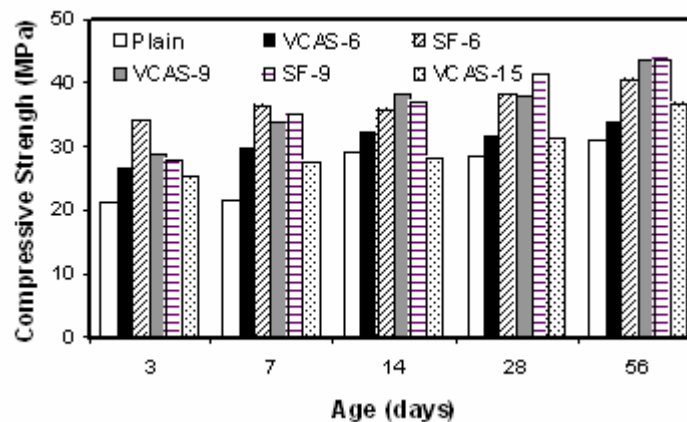


(b) w/b = 0.50

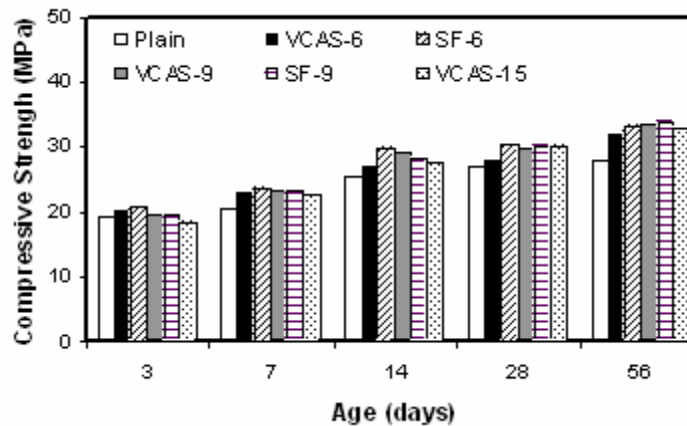
FIGURE 6 Free shrinkage of concretes with w/b of: (a) 0.40, (b) 0.50.

Free Shrinkage Strains of VCAS and SF Modified Concretes

The free shrinkage strains of the concrete mixtures at 3, 7, 14 and 28 day ages are shown in Fig. 6(a) and 6(b) for 0.40 and 0.50 w/b mixtures respectively. It can be seen that the addition of both the pozzolans increased the free shrinkage in all the concrete mixtures, especially at later ages (7 days and later). Researchers in the past have observed similar increase in shrinkage strains due to the addition of silica fume (12,13,14) and high reactivity metakaolin (13) in concrete. They found that the addition of these highly reactive pozzolans increased the autogenous shrinkage of concrete mixtures resulting in higher overall shrinkage. It is also evident from Figs. 6(a) and (b) that a decrease in w/b from 0.50 to 0.40 resulted in increases in shrinkage in all the mixtures. This increase in overall free shrinkage can be attributed to the fact that a decrease in w/b can result in an increase in autogenous shrinkage in the mixtures while paste content remains the same (15).



(a) w/b = 0.40



(b) w/b = 0.50

FIGURE 7 Compressive strengths of concretes with w/b of: (a) 0.40, (b) 0.50.

Compressive Strength

The development of compressive strengths in 0.40 and 0.50 w/b mixtures are shown in Figs. 7(a) and 7(b). The concrete mixtures containing either VCAS or SF demonstrates higher strength from an early age (3 days). This facilitates the incorporation of these pozzolans in

transportation structures such as concrete pavements and bridge decks, where a high early strength attainment can prevent delay in construction that might cause significant inconvenience to the public (14). The increase in strength in concretes containing VCAS and SF can be explained by the fact that these pozzolans play an important role in improving the aggregate-paste bond through the densification of the transition zone and the formation of more calcium silicate hydrates due to pozzolanic reactions (16, 17). The observed high early age strength can be attributed to the high pozzolanic reactivity of these pozzolans due to their finer particle sizes, and the fine filler effect.

Resistance to Chloride Penetration

Fig. 8(a) shows the rapid chloride permeability (RCP) values of w/b 0.40 concretes incorporating 6, 9, and 15% of VCAS after 28 and 45 days of moist curing, while Figure 8(b) shows the RCP values for concrete mixtures with 6 and 9% SF. The control concrete can be seen to have a high chloride permeability (> 4000 coulombs) after 28 days of moist curing and moderate permeability (> 2000 coulombs) after 45 days of moist curing. From both these figures, it can be seen that increasing the dosage of either VCAS or SF in concrete results in a reduction in the RCP values. With increasing curing duration, the reduction in RCP values of the concretes with VCAS or SF is greater than those of the control concrete, providing indication of the densification of the material microstructure of modified concretes. After 45 days of curing, concretes containing 6% SF and 9% VCAS were found to perform similarly with respect to their chloride ion penetrability, both showing low RCP values (< 2000 coulombs). The same could be said about concretes containing 9% SF and 15% VCAS, which show very low RCP values (< 1000 coulombs). For the same replacement level of cement, SF concretes demonstrates a higher reduction in RCP values at the ages considered in this study.

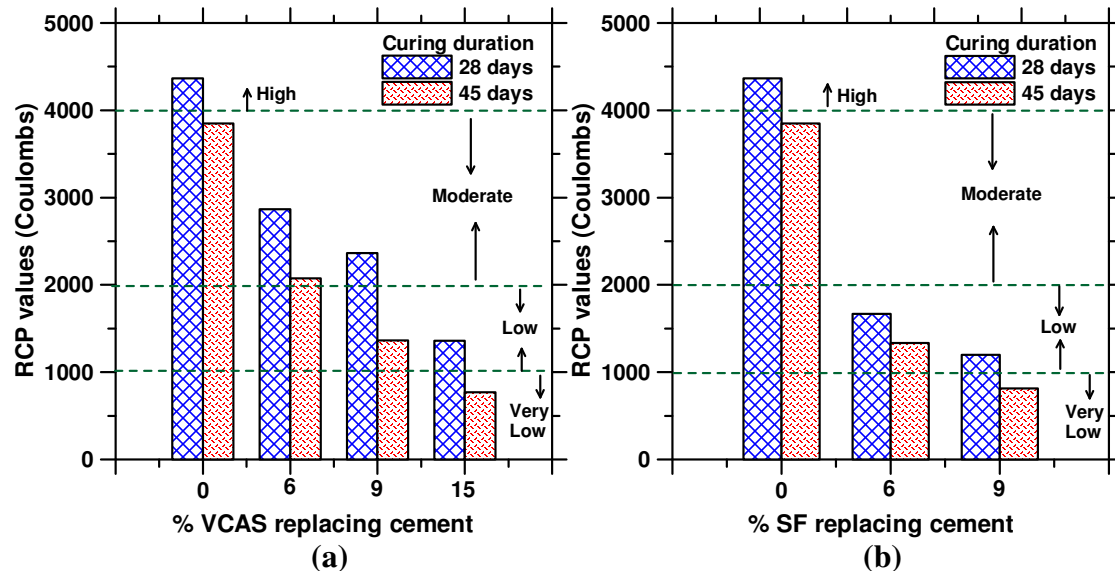


FIGURE 8 RCP values of concretes containing: (a) VCAS, (b) SF.

Moisture Transport through VCAS and SF Modified Concretes

The water transport through mortars and concrete is typically defined using the sorptivity coefficient (18,19). Since sorption dictates only the short-term water intake by concrete specimens, and diffusion dominates the long-term intake, recent studies have described the overall water transport in mortars and concrete using a sorption-diffusion approach (20, 21). In this approach, the classical equation for sorption based on parallel tube model of porous media is modified by adding another term to account for the diffusion of moisture into the specimen. The solution of the Fickian diffusion equation for a cylindrical rod with one end sealed and the other end maintained at the same concentration throughout is used for diffusive transport. The combined equation for moisture transport using this model (21) is expressed as:

$$\left(\frac{M}{A}\right)_t = B\left[1 - \exp\left(-\frac{St^{1/2}}{B}\right)\right] + C_0L\left\{1 - \sum_{n=0}^{\infty} \frac{8}{(2n+1)^2\pi^2} \exp\left[-\frac{D_m(2n+1)^2\pi^2t}{4L^2}\right]\right\} \quad (3)$$

$(M/A)_t$ is the normalized moisture intake (M is the mass of water absorbed by a specimen of surface area A) at any time t , S is the sorptivity, D_m is the moisture diffusion coefficient, B is a constant related to the distance from the absorbing surface over which the capillary pores dominate the initial sorption, and C_0 is the constant surface concentration of the diffusing species. The first term in the equation represents the capillary intake of water through the larger pores, and the second term represents the moisture diffusion through smaller pores, including the gel pores. By fitting Eq. 3 to the data of normalized moisture intake over time, the coefficients B , S , C_0 , and D_m could be obtained.

Figs. 9(a) and (b) depict the normalized water intake over time for VCAS and SF modified concretes respectively. The symbols in these figures represent the experimental data and the smooth lines represent the fit of Equation 3 to the data. Equation 3 is found to fit the experimental data very well with R^2 values around 0.99 for all the cases. Table 3 shows the values of the parameters as determined from the fit of this model to the experimental data. To facilitate easier convergence of results, the value of sorptivity (S) in Equation 3 has been set as the slope of the plot of normalized water intake curve against the square root of time over a period of first 24 hours. Though it has been proved that the sorptivity values thus determined are lower (18) by about 10-20% than the long-term sorptivity for specimens saturated as described in this paper, such a compromise is justified by the relative closeness of the other model parameters thus determined to the corresponding values obtained when S is unconstrained.

From Figs. 9(a) and (b), it can be seen that, for concretes containing higher proportions of VCAS and SF, the total moisture intake after a period of 400 hours or more is lower than the corresponding value for the control concrete. However, for mixtures containing 6% of VCAS or SF, the total moisture intake is similar to or slightly higher than that of the control concrete. The explanation for this behavior is given in the context of the parameters of the model.

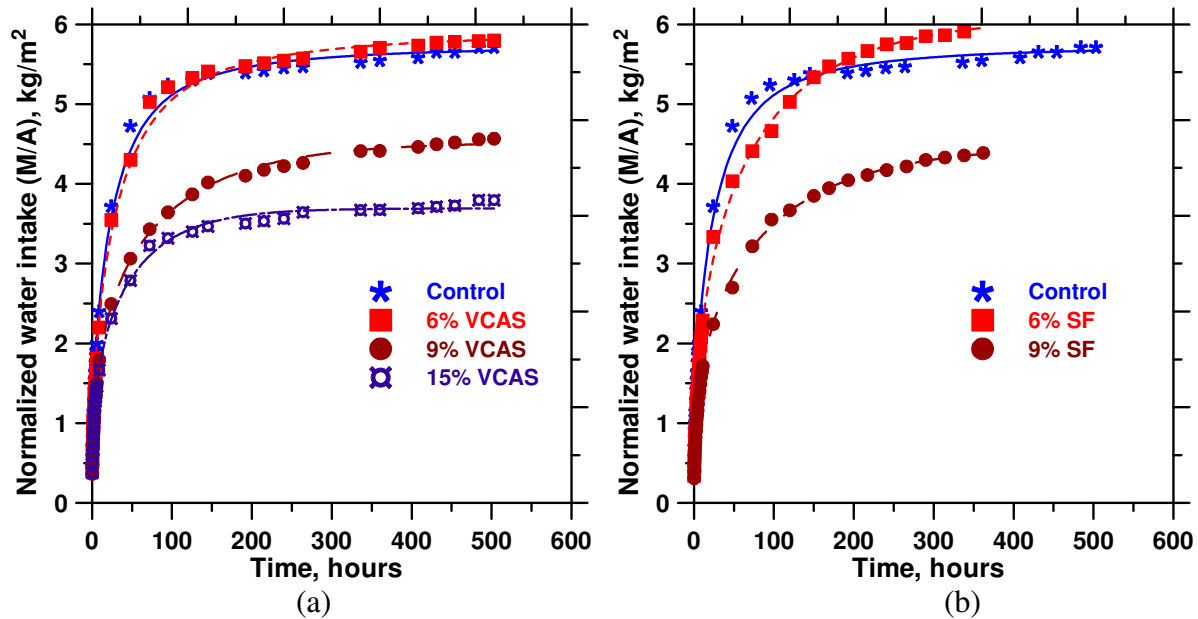


FIGURE 9 Normalized water intake for concretes containing: (a) VCAS, (b) SF.

From Table 3, it can be observed that the sorptivity values decrease with increase in both VCAS and SF dosages. The reduction is found to be higher with increase in SF dosage, indicating the higher efficiency of SF in reducing sorptivity. Since sorption is primarily due to the water intake through the larger capillary pores (18), a reduction in sorptivity obviously indicates pore size refinement. However, the sorptivity values should not be seen in isolation from the values of the constant B , which provides an indication of the depth from the absorbing face over which the capillary pores dominate sorption. It can be noticed from Table 3 that the value of constant B is slightly higher for mixtures containing 6% VCAS or SF as compared to that of control concrete. Though the sorptivity values of these mixtures are lower than that of control concrete, a slightly higher value of B results in higher water intake during the early hours of exposure. This explains the slightly higher overall moisture intake of mixtures with 6% VCAS or SF as compared to control concrete. The reason for the slightly higher values of B for these mixtures is explained as follows. For the mixtures with 6% VCAS or SF, there is evidently pore size refinement as indicated by their lower S values. But these capillary pores still transport water by sorption though a little slowly, as shown by the lower S values. It is also seen from the moisture intake curves that these specimens take in more water during the early hours of exposure. Hence, higher moisture intake, but a lower sorptivity means that B has to be slightly larger. Accounting for the pore size refinement that is well known when using such replacement materials, the higher B can only be explained by the fact that there is not much reduction in the connectivity of the sorption controlled pore sizes (this does not mean that the overall pore connectivity is not reduced). Further tests are necessary to confirm this postulation. As the proportion of either VCAS or SF further increases, the value of B reduces, because of both pore size refinement and reduced pore connectivity. These factors also contribute to the reduced sorptivity, and eventually the reduced overall moisture intake of mixtures with high proportions of VCAS or SF.

From Table 3, it can be noticed that the surface concentration values (C_0) are similar for all the mixtures investigated. C_0 is primarily a function of the saturation level of the

specimen before the test (20), and since all the specimens tested have similar saturation levels (they were subjected to the same pre-conditioning treatment), it is not surprising that their C_0 values are similar. A general reduction in the diffusion coefficient values with increasing VCAS or SF contents can also be observed, attributable to the reduced pore volume and lower proportion of diffusion-dominant pore sizes (as a result of reduced total pore volume) in these mixtures. However, for the mixture with 15% VCAS, the diffusion coefficient is found to be higher than that of the mixture with 9% VCAS. The reason for this behavior is as follows. The S values are lowest for the mixture with 15% VCAS indicating that there is a high degree of pore size refinement. The lower B values show that the depth to which sorption controls the transport process is also small, which means that diffusion starts earlier for this mixture. Though the overall pore volume is expected to be less for this mixture than that for a 9% VCAS mixture, it is conceivable that there is a higher proportion of diffusion-dominant pore sizes in the 15% VCAS mixture because of the above-mentioned reason, resulting in a higher diffusion coefficient.

TABLE 3 Parameters of the Fit of Equation 3 to the Moisture Intake Data

Replacement material	% replacing cement	Parameters from the fit of sorption-diffusion equation			
		B (mm)	S (kg/m ² hr ^{0.5})	C ₀ (kg/m ³)	D _m (m ² /hr)
None	0	4.02	0.80	33.91	3.31*10 ⁻⁵
VCAS	6	4.26	0.74	32.62	2.66*10 ⁻⁵
	9	2.56	0.64	39.33	0.92*10 ⁻⁵
	15	1.73	0.62	39.32	1.55*10 ⁻⁵
SF	6	4.16	0.69	39.85	1.11*10 ⁻⁵
	9	2.58	0.52	38.34	0.87*10 ⁻⁵

CONCLUSIONS

Based on the results of the experimental investigations described in this paper, the following conclusions are drawn:

- (i) VCAS increases the slump of fresh concrete mixtures indicating a low water demand, while SF reduces the slump. Due to its reduced water demand, VCAS can be used to proportion concretes of lower w/b, or with higher cement replacement levels, both of which impacts the long term performance of structures beneficially.
- (ii) Concrete mixtures containing VCAS shows lower plastic shrinkage cracking than SF mixtures. This beneficial property can help alleviate one of the major problems in the construction of transportation structures such as bridge decks and pavements.
- (iii) Addition of VCAS and SF increases the free shrinkage of concrete. Therefore, proper precautions (i.e., use of external or internal curing methods, use of shrinkage reducing admixture etc.) should be taken if these highly reactive pozzolans are to be used in concretes for bridge decks, pavements and other concrete structures that have a tendency to develop shrinkage cracking.
- (iv) Both VACS and SF increases the short and long term compressive strength of concrete. Therefore VCAS, like SF, offers tremendous potential for use in transportation structures where both short and long term strengths are important.
- (v) Incorporation of VCAS or SF as a replacement of cement results in increased chloride penetration resistance of the concretes. At equal replacement levels, the beneficial

effect is higher with SF addition. After 45 days of moist curing, there is no difference between the RCP values of concretes with 9% SF and 15% VCAS.

- (vi) An increase in VCAS or SF dosage is generally observed to reduce the total amount of moisture absorbed by the concretes. The sorptivity reduces with increase in VCAS or SF content, the reduction being more prominent with SF addition. The depth to which the capillary pores control sorption, as well as the moisture diffusion coefficient also show a general decreasing trend with increasing VCAS or SF content. In all of these cases, under the curing duration investigated, SF mixtures show drastic reduction than the VCAS mixtures, demonstrating their effectiveness in pore size refinement. The mixture with 15% VCAS show comparable sorptivity and moisture diffusion coefficient to that of the 6% SF mixture. Increased dosages of VCAS (of the order of 20 or 25% as is commonly used for fly ash) is anticipated to result in performance characteristics similar to that of 9-10% SF, which is part of an ongoing investigation.

REFERENCES

1. Miller, R., T.M. Baseheart, and R. Sprague. Use of High-Performance Concrete for Bridge Abutment. In *Transportation Research Record: Journal of the Transportation Research Board, No.1740*, TRB, National Research Council, Washington, D.C., 2000, pp. 19-24.
2. Malhotra, V.M., and P.K. Mehta. Pozzolanic and Cementitious Materials, *Advances in Concrete Technology*, Gordon and Breach, London, 1996.
3. Hassan, K.E., J.G. Cabrera, and R.S. Maliehe. The effect of Mineral Admixtures on the Properties of High-Performance Concrete. *Cement and Concrete Composites*, V.22, 2000, pp. 267– 271.
4. Hemmings, R. Process for Converting Waste Glass Fiber Into Value –Added Products, DOE Report No. DE-FG36-03GO13015, Albacem, LLC., 2005.
5. ASTM (1994). *Annual Book of ASTM Standards, Concrete and Aggregates, Vol. 4.02*, © 1994.
6. Qi, C, J. Weiss, and J. Olek. Characterization of Plastic Shrinkage Cracking in Fiber Reinforced Concrete Using Image Analysis and a Modified Weibull Function, *Materials and Structures*, V. 36, No. 6, 2003, pp. 386-395.
7. Qi, C, J. Weiss, and J. Olek. Statistical Significance of the Restrained Slab Test for Quantifying Plastic Cracking in Fiber Reinforced Concrete, *Journal of ASTM International*, v.2, no.7, 2005.
8. Gopalan, M.K. Sorptivity of Fly Ash Concretes, *Cement and Concrete Research*, Vol 26, 1996, pp. 1189-1197.
9. Khatib, J.M., and R.M. Clay. R.M. Absorption Characteristics of Metakaolin Concrete, *Cement and Concrete Research*, Vol 34, 2004, pp. 19-29.
10. RILEM TC 116-PCD: Permeability of Concrete as a Criterion of its Durability - Tests for Gas Permeability of Concrete C. Determination of the Capillary Absorption of Water of Hardened Concrete, *Materials and Structures*, V.32, No. 217, 1999, pp. 174-179.
11. Garon R.J., N.C. Wong, and P. Balaguru. Influence of Silica Fume and Refined Pozzolan on Plastic Shrinkage Cracking of Concrete. Report No: 99-10, Boral Material Technologies, July 1999.

12. Subramaniam, K.V., R. Gromotka, S.P. Shah, K. Obla, and R.L. Hill. Influence of Ultrafine Fly Ash on the Early Age Response and the Shrinkage Cracking Potential of Concrete. *ASCE Journal of Materials in Civil Engineering*, January/February, 2005, pp. 45-53.
13. Hossain, A.B., S. Islam and B. Reid. A Comparative Study on Mortar Containing Silica Fume and High Reactivity Metakaolin in Relation to Restrained Shrinkage Stress Development and Cracking, *ACI SP-242: 9th CANMET/ACI International Conference on Fly Ash, Silica Fume, Slag and Natural Pozzolans in Concrete*, Warsaw, Poland, 2007, pp. 187-198.
14. Hossain, A.B., S. Islam and K. Copeland. Influence of Ultrafine Fly Ash on The Shrinkage and Cracking Tendency of Concrete and the Implications for Bridge Decks, *Proceedings of the 86th Transportation Research Board Annual Meeting*, Washington, D.C., January 2007.
15. Hossain, A. B., and W.J. Weiss. Assessing Residual Stress Development and Stress Relaxation in Restrained Concrete Ring Specimens. *Cement and Concrete Composites*, V.26, 2004, pp. 531-540.
16. Shannag, M.J. High strength concrete containing natural pozzolan and silica fume, *Cement and Concrete Research*, V.22, 200, pp. 399-406.
17. Goldman, A. and A. Bentur. Bond Effects in High Strength Silica Fume Concretes. *ACI Materials Journal*, Vol 86, 1989; pp.440-447.
18. Martys, N.S., and C.F. Ferraris. Capillary Transport in Mortars and Concrete, *Cement and Concrete Research*, Vol. 27, No. 5, 1997, pp. 747-760.
19. Hall, C., Water Sorptivity in Mortars and Concrete: A Review, *Magazine of Concrete Research*, Vol 41, No. 147, 1989, pp. 51-61.
20. Neithalath, N. Analysis of moisture transport in mortars and concrete using sorption-diffusion approach. *ACI Materials Journal*, Vol. 103, 2006, pp. 209-217.
21. Neithalath, N. Evaluating the short- and long-term moisture transport phenomena in lightweight aggregate concretes, *Magazine of Concrete Research*, Vol 59, 2007, pp. 435-445.